RAFT Homo- and Copolymerization of *N*-Acryloyl-morpholine, Piperidine, and Azocane and Their Self-Assembled Structures

Yun Suk Jo,[†] André J. van der Vlies,[†] Jay Gantz,[†] Sasa Antonijevic,[‡,||] Davide Demurtas,[§] Diana Velluto,[†] and Jeffrey A. Hubbell[†,‡,*]

Institute of Bioengineering (IBI) and Institute of Chemical Sciences and Engineering (ISIC), École Polytechnique Fédérale de Lausanne (EPFL), Lausanne CH 1015, Switzerland, and Centre Intégratif de Génomique, Faculté de Biologie et de Médecine, Université de Lausanne, CH-1015 Lausanne, Switzerland

Received July 31, 2007; Revised Manuscript Received December 19, 2007

ABSTRACT: We present new polymeric amphiphiles derived from *N*-acryloyl derivatives of the cyclic secondary amines: morpholine, piperidine, and azocane polymerized by reversible addition−fragmentation transfer (RAFT) polymerization. Both homopolymerization and block copolymerization of *N*-acryloylmorpholine (AM), *N*-acryloylpiperidine (AP), and *N*-acryloylazocane (AH) were carried out. The block copolymeric amphiphiles, poly[(*N*-acryloylmorpholine)-*block*-(*N*-acryloylpiperidine)] (PAM-PAP) and poly[(*N*-acryloylmorpholine)-*block*-(*N*-acryloylazocane)] (PAM-PAH) were investigated, PAM being a hydrophile, and PAP and PAH being hydrophobes. Moreover, to compare PAM as a hydrophilic block with poly(ethylene glycol) (PEG), poly[(ethylene glycol)-*block*-(*N*-acryloylpiperidine)] (PEG-PAP) was also formed. In all cases, the degree of polymerization was well-controlled and polymers were obtained in monomodal distributions. The macroamphiphile aggregates in water were reproducibly well-formed by dialysis with a size range between 10 and 70 nm as characterized by dynamic light scattering (DLS). The morphology of the aggregates was examined by transmission electron microscopy (TEM). All aggregates formed from PAM-PAP and PAM-PAH series, up to 0.76 and 0.85 hydrophobic weight fraction, respectively, revealed spherical micelles, whereas coexistence of spherical micelles and/or polymersomes was observed from PEG-PAP at a hydrophobic weight fraction of 0.91. From study of copolymer segregation behavior, PEG-PAP and PAM-PAH span the weak segregation region (WSR) as well as the strong segregation region (SSR), whereas PAM-PAP is positioned in the WSR, owing to the greater hydrophobicity of PAH than PAP. PAM yielded similar aggregation results to PEG when copolymerized with hydrophobic blocks. As a model drug, everolimus was loaded in PAM(0.15)-PAH(0.85) micelles. After loading the drug, the micelle hydrodynamic diameter was slightly increased from 43 ± 0.1 to 52 ± 1.8 nm. Everolimus was encapsulated with 60 ± 7.8% of efficiency and was released over 3 wk in PBS (pH 7.4, 10 mM) at 37 °C.

1. Introduction

Polymeric aggregates are widely studied as drug delivery systems (DDS) in biomedical research because they can solubilize hydrophobic drugs within their hydrophobic cores and can also be suitable platforms as prodrugs by covalent conjugation of drugs with degradable spacers.[1−4] Polymeric amphiphiles form self-assembled aggregates with different topologies including spherical micelles, wormlike micelles, and bilayer vesicles (polymersomes).[5−11] Nanosized micelles allow drugs to penetrate tumors with reduced toxicity to nontumor tissue by virtue of the enhanced permeation and retention (EPR) effect, derived from the leakiness of the tumor vasculature.[12,13] Thus, much research has been done to design appropriate amphiphilic copolymers to load a number of drugs such as adriamycin,[14−17] camptothecin,[18−21] paclitaxel,[22−26] cyclosporine A,[27−29] cisplatin,[30,31] and others.[32,33]

As a suitable polymer for DDS, poly(ethylene glycol) (PEG) is widely accepted as a hydrophilic domain, or simply for the modification of biomolecules, referred to as "PEGylation", endowing many favorable "stealthy" effects to various substrates.[34−38] Similarly, poly(*N*-acryloylmorpholine) (PAM) is considered as another candidate for the same purposes. In several studies, PAM has shown low toxicity and a low incidence of provoking immunological reactions *in vivo*.[39−42] For example, as Torchilin and co-workers noted,[41,42] PAM-modified liposomes showed prolonged in-blood residence time after *in vivo* administration. For this reason, PAM can be regarded as another hydrophilic polymer suitable for DDS.

PAM has been generally synthesized by free radical polymerization,[43,44] yet recently there have been several studies examining the synthesis of PAM by living radical polymerization (LRP) techniques.[45−48] Polymers prepared by LRP often have low polydispersity with high monomer conversion, even under mild reaction conditions. Another important advantage of LRP is the ability to subsequently add another building block to the "living" terminus of a previously polymerized chain. Thus, to achieve well-defined block copolymers, LRP appears as a very attractive technique. Among LRP techniques, reversible addition−fragmentation transfer (RAFT) polymerization has been extensively studied for the homo- and copolymerization of (meth)acrylamides,[49−52] since it was first reported.[53] In comparison to other LRPs, one of the biggest advantages of RAFT polymerization is its versatility in polymerizing diverse

* To whom correspondence should be addressed: E-mail: jeffrey.hubbell@epfl.ch. Telephone: +41 21 693 9681. Fax: +41 21 693 9665.

[†] Institute of Bioengineering (IBI), École Polytechnique Fédérale de Lausanne (EPFL).

[‡] Institute of Chemical Sciences and Engineering (ISIC), École Polytechnique Fédérale de Lausanne (EPFL).

[§] Centre Intégratif de Génomique, Faculté de Biologie et de Médecine, Université de Lausanne.

[||] Current address: Department of Chemistry, University of California, Berkeley, and Division of Materials Science, Lawrence Berkeley National Laboratory, Berkeley, California 94720.

10.1021/ma071710t CCC: $40.75
Published on Web 02/05/2008

monomers.[49,54−56] For instance, olefins, vinyl halides, and vinyl acetates are not amenable to atom transfer radical polymerization (ATRP) due to an equilibrium constant during polymerization that is too low, yet are readily polymerized via RAFT.[56,57] For poly(acrylamide) synthesis, despite some outstanding results,[58−60] ATRP is still not regarded as suitable a method as RAFT polymerization because of its high polydispersity and poor monomer conversion.

We sought to explore the aggregation behavior of block copolymeric amphiphiles with PAM as a hydrophile, and thus we sought hydrophobic monomers of structure analogous to morpholine: there exists another 6-membered cyclic secondary amine, piperidine. *N*-acryloylpiperidine (AP), prepared by acylation of piperidine, can be polymerized to poly(*N*-acryloylpiperidine) (PAP) by radical polymerization. However, different from PAM, PAP undergoes phase transition at 4−6 °C and remains hydrophobic above this lower critical solution temperature (LCST).[61] Furthermore, there are other analogues of piperidine with different numbers of methylene groups on the aliphatic ring, such azocane (Syn: heptamethyleneamine, 8-membered ring), from which a still more hydrophobic monomer could be synthesized. Thus, *N*-acryloylazocane (AH) was also polymerized to poly(*N*-acryloylazocane) (PAH) by RAFT. Furthermore, to block copolymerize AP and AH with the hydrophilic block PAM by RAFT, we employed PAM as a macromolecular chain transfer agent (CTA); PEG was similarly employed, to compare these two hydrophilic polymer blocks. Three amphiphilic diblock copolymers were synthesized in combining the four building blocks: PEG, PAM, PAP, PAH, namely poly[(ethylene glycol)-*block*-(*N*-acryloylpiperidine)] (PEG-PAP), poly[(*N*-acryloylmorpholine)-*block*-(*N*-acryloylpiperidine)] (PAM-PAP), and poly[(*N*-acryloylmorpholine)-*block*-(*N*-acryloylazocane)] (PAM-PAH).

From the amphiphilic diblock copolymers synthesized in this work, the effect of different hydrophiles and hydrophobes on the size of aggregates and their segregating behaviors was studied. The synthesized polymers were fully characterized by ^{1}H NMR, ^{13}C NMR, and size exclusion chromatography (SEC). The aggregates formed from the resulting diblock copolymers were characterized by dynamic light scattering (DLS), the evaluation of critical micelle concentration (cmc), and transmission electron microscopy (TEM). A model hydrophobic drug, everolimus was loaded in PAM-PAH micelles and its release profile was monitored with a SEC module equipped with photodiode array detector (PDA).

2. Experimental Section

2.1. Materials. Chemicals were used as received unless stated otherwise. 2-Bromopropionic acid (99+%), phenylmagnesium chloride solution in tetrahydrofuran (THF) (2.0 M), carbon disulfide (99+%), 2-chloro-2-phenylacetyl chloride (CPAC, 90%), Na_2SO_4 (99%), KOH (85+%), and $NaHCO_3$ (99.5%) were purchased from Sigma-Aldrich (Steinheim, Germany). Morpholine (99+%), piperidine (98%), azocane (97+%), CaH_2 (95+%), $LiAlH_4$ (97+%), 2,2′-azobis(2-methylpropionitrile) (AIBN) (98+%), $KMnO_4$ (99+%), $KHSO_4$ (98+%) K_2CO_3 (99+%), ninhydrin (99%), PEG monomethyl ether ($\overline{M}_n$ = 2 kDa), and acryloyl chloride (96+%) were purchased from Fluka (Buchs, Switzerland). Everolimus was a gift from Guidant AVS. AIBN was recrystallized twice from methanol. Triethylamine (TEA) (99%) was purchased from Acros (Geel, Belgium) in biochemical grade. TEA was distilled over CaH_2 and stored at −20 °C until used. Solvents were purchased from various suppliers in reagent grade or HPLC grade. Solvents were used without purification unless stated otherwise. 1,4-dioxane was distilled over $LiAlH_4$ and THF was distilled over KOH. Distilled solvents were stored over molecular sieves at room temperature until used. NMR solvents ($CDCl_3$, DMSO-d_6) and tetramethylsilane (TMS) were purchased from Armar chemicals (Döttingen, Switzerland) with 99.8% purity. Argon gas was purchased from Messer Schweiz AG (Préverenges, Switzerland). Phosphate buffered saline (PBS) solution (pH 7.4, 10 mM) was prepared in Milli-Q water according to the standard protocol.

Scheme 1. Monomer Synthesis: *N*-Acryloylmorpholine (AM, 1), *N*-Acryloylpiperidine (AP, 2), and *N*-Acryloylazocane (AH, 3)

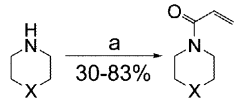

a: CH_2Cl_2, 0 °C / r.t., 2-4 h

1: X = O (30%)
2: X = CH_2 (81%)
3: X = $CH_2CH_2CH_2$ (83%)

2.2. Characterization and Analysis. Purification by column chromatography was done using 230−400 mesh MN 60 silica gel (Macherey Nagel, Düren, Germany). Thin layer chromatography (TLC) was done using silica gel 60 F254 coated aluminum sheets (Merck KGaA, Darmstadt, Germany). TLC plates were colored with ninhydrin (to detect amines) or $KMnO_4$ (to detect substances prone to oxidation such as acrylamides, amines, etc.) solutions after visualization under UV light (λ_{ABS} = 254 nm). For the ninhydrin assay, the TLC plate was heated with a butane torch or an electric heat gun. Solution ^{1}H NMR (400 MHz) spectra were recorded on a Bruker 400 UltraShield spectrometer at room temperature. NMR relaxation delay was set to 10 s for all samples with 32 scans for ^{1}H NMR spectra. Chemical shift values (δ) of ^{1}H are reported in ppm relative to TMS as an internal standard. Solid-state ^{13}C{^{1}H} CPMAS NMR (75 MHz) spectra were recorded on a Bruker DRX 300 spectrometer equipped with 7.0 T widebore magnet and 4 mm CPMAS probe head. Finely powdered samples were packed into 4 mm outer diameter ZrO_2 rotors and measured with a spin rate of 10 kHz. Two-pulse phase modulation (TPPM)[62] proton decoupling was used for signal acquisition. The spectra are the result of averaging 640 transients with a recycle interval of 5 s. The cross-polarization contact time was 1 ms. Chemical shifts of ^{13}C are reported in ppm and given relative to TMS as external standard. $\overline{M}_w$ denotes the weight-average molecular weight and $\overline{M}_n$ denotes the number-average molecular weight. Polydispersity (PD = $\overline{M}_{w(SEC)}/\overline{M}_{n(SEC)}$) was obtained by size exclusion chromatography (SEC), for which *N*,*N*′-dimethylformamide (DMF) or THF was used as an eluent. When DMF was used, a Waters Alliance GPCV 2000 with a light scattering detector was used in addition of LiCl to the eluent with 0.5 g/L of concentration. The flow rate was 0.5 mL/min at 60 °C. When THF was used, no salt was added to the eluent (flow rate: 1 mL/min) and a Waters Alliance 2695 Separation Module was used with miniDAWN (Wyatt Technology, Santa Barbara, CA). Operating temperature was maintained at 40 °C. UV/vis measurements and cmc determinations were done either with a Tecan SAFIRE^2 microplate reader using 96-well microplate or a Shimadzu UV mini 1240 spectrometer using a quartz cuvette. $\overline{M}_{n(UV/vis)}$ was determined by measuring the absorbance of phenyl dithioester groups at the end of polymer chains at 496 nm. A calibration curve was obtained from different concentration of CTA. Mass spectra were obtained using Waters Micromass ZQ instrument with ESI+ (capillary voltage: 3.0 kV) or APCI+ (corona current: 8.0 μA) ionization modes.

2.3. Synthesis.

2.3.1. Monomer Synthesis (Scheme 1). The monomers were obtained with purity higher than 95% with negative reaction by ninhydrin to confirm that no free amine exists. Once synthesized, monomers were protected from the light and kept at −20 °C prior to polymerization.

2.3.1.1. *N*-Acryloylmorpholine (AM, 1). The synthetic procedures were referred to as reported earlier with some modifications.[63] A solution of acryloyl chloride (0.2 mol, 16.0 mL) in CH_2Cl_2 (250

mL) was slowly added to a solution of morpholine (0.4 mol, 35.0 g) in CH_2Cl_2 (500 mL) previously cooled at 0 °C. After 1 h, all acryloyl chloride had been added and the white suspension was warmed to room temperature. After 3 h at room temperature, the mixture was concentrated under reduced pressure to about 300 mL and filtered to remove the morpholine·HCl salt and rinsed with small volumes of CH_2Cl_2. The filtrate was successively washed with H_2O (100 mL), $KHSO_4$ (aq, 1 M, 100 mL), H_2O (100 mL), $NaHCO_3$ (aq, 5% (w/v), 100 mL), and H_2O (100 mL). The clear solution was dried over Na_2SO_4, and concentrated under reduced pressure at 30−40 °C to yield clear colorless or pale yellow oil.

Yield: 30%. TLC (EtOAc, SiO_2): R_f = 0.34. ^{1}H NMR (400 MHz, $CDCl_3$): δ 6.57 (dd, 1H, C**H**═CH_2), 6.30 (d, 1H, CH═C**H**$_{trans}$), 5.72 (d, 1H, CH═C**H**$_{cis}$), 3.69 (s, 4H, C**H**$_2$-O), 3.58 (s, 4H, C**H**$_2$-N); MS (*m*/*z*, M + H$^+$, APCI+): 142.1.

2.3.1.2. *N*-Acryloylpiperidine (AP, 2). The synthetic procedures were referred to as reported earlier with some modifications.[61] A solution of acryloyl chloride (0.025 mol, 2.0 mL) in CH_2Cl_2 (50 mL) was added to a solution of piperidine (0.05 mol, 5.0 mL) in CH_2Cl_2 (100 mL) previously cooled at 0 °C After 30 min, all acryloyl chloride had been added and the white suspension was warmed to room temperature. After 2 h at room temperature, the mixture was filtered and white residue was washed with CH_2Cl_2 (25 mL). Purification was done as described above for AM. The clear solution was dried over Na_2SO_4, and concentrated under reduced pressure at 30−40 °C to yield a clear colorless or pale yellow oil.

Yield: 81%. TLC (EtOAc): R_f = 0.40. ^{1}H NMR (400 MHz, $CDCl_3$): δ 6.59 (dd, 1H, C**H**═CH_2), 6.24 (d, 1H, CH═C**H**$_{trans}$), 5.65 (d, 1H, CH═C**H**$_{cis}$), 3.63−3.60 (m, 4H, C**H**$_2$-N), 1.69−1.64 (m, 4H, C**H**$_2$), 1.59−1.55 (m, 2H, C**H**$_2$); MS (*m*/*z*, M + H$^+$, ESI+): 140.1.

2.3.1.3. *N*-Acryloylazocane (AH, 3). A solution of acryloyl chloride (0.044 mol, 3.54 mL) in CH_2Cl_2 (50 mL) was added to a solution of azocane (0.04 mol, 5.0 mL) and TEA (0.04 mol, 5.51 mL) in CH_2Cl_2 (200 mL) previously cooled at 0 °C After 1 h, all acryloyl chloride had been added and warmed to room temperature. After 1 h, the organic solution was washed as was done for AM, described above. The clear solution was dried over Na_2SO_4, and concentrated was under reduced pressure at 30−40 °C to yield clear colorless or pale yellow oil.

Yield: 83%. TLC (EtOAc): R_f = 0.41. ^{1}H NMR (400 MHz, $CDCl_3$): δ 6.60 (dd, 1H, CH═C**H**$_2$), 6.34 (d, 1H, CH═C**H**$_{trans}$), 5.66 (d, 1H, CH═C**H**$_{cis}$), 3.59−3.46 (m, 4H, C**H**$_2$-N), 1.82−1.69 (m, 4H, C**H**$_2$), 1.64−1.47 (m, 6H, C**H**$_2$). MS (*m*/*z*, M + H$^+$, ESI+): 168.1.

2.3.2. 2-[(2-Phenyl-1-thioxo)thio]propanoic Acid (Chain Transfer Agent, CTA). The procedure was followed as reported by D'Agosto et al.[45] except that the Grignard reagent was replaced with phenylmagnesium chloride and excess 2-bromopropionic acid was removed using a conventional distillation setup. In addition, a different eluent composition was used for purification by column chromatography: ethyl acetate/*n*-hexane/acetic acid (20:80:1). After column chromatography, solvent was removed under reduced pressure and the red oil was crystallized from *n*-hexane to yield red-orange crystals.

Yield: 47%. TLC (EtOAc): R_f = 0.38. ^{1}H NMR (400 MHz, $CDCl_3$): δ 8.10−7.90 (m, 2H, Ar**H**), 7.55 (m, 1H, Ar**H**), 7.48−7.34 (m, 2H, Ar**H**), 4.81 (q, 1H, C**H**), 1.72 (d, 3H, C**H**$_3$). MS (*m*/*z*, M + H$^+$, ESI+): 227.0.

2.3.3. Homopolymers: Poly(*N*-acryloylmorpholine) (PAM, 4a), Poly(*N*-acryloylpiperidine) (PAP, 4b), and Poly(*N*-acryloylazocane) (PAH, 4c) (Scheme 2). The respective monomer (10.8 mmol, 1.52 g of AM, 1.50 g of AP, 1.81 g of AH), CTA (0.22 mmol, 49.8 mg) and AIBN (0.022 mmol, 3.61 mg) were loaded in a Schlenk tube and mixed in 1,4-dioxane (5 mL). After the tube was closed with a silicone septum, the solution was subjected to five freeze−thaw cycles under vacuum (20−50 mbar). Polymerization was carried out at 90 °C for 24 h and the polymers were precipitated in cold *n*-hexane or diethyl ether. After the filtration, the polymers were dried *in vacuo*.

Scheme 2. Homopolymerization: Poly(*N*-acryloylmorpholine) (PAM, 4a), Poly(*N*-acryloylpiperidine) (PAP, 4b), and Poly(*N*-acryloylazocane) (PAH, 4c)

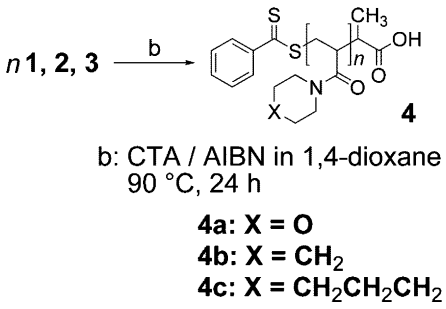

Scheme 3. Diblock Copolymerization I: Poly[(*N*-acryloylmorpholine)-*block*-(*N*-acryloylpiperidine)] (PAM-PAP, 5a) and Poly[(*N*-acryloylmorpholine)-*block*-(*N*-acryloylazocane)] (PAM-PAH, 5b)

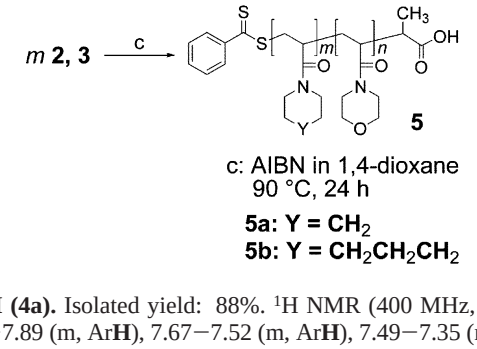

PAM (4a). Isolated yield: 88%. ^{1}H NMR (400 MHz, $CDCl_3$): δ 8.05−7.89 (m, Ar**H**), 7.67−7.52 (m, Ar**H**), 7.49−7.35 (m, Ar**H**), 5.23−5.04 (m, C**H**), 4.01−3.10 (m, C**H**$_2$), 2.82−2.13 (m, C**H**), 1.99−1.02 (m, C**H**$_2$). ^{13}C{^{1}H} CPMAS NMR (75 MHz): δ 173.5 (s, N−**C**═O), 67.0 (s, **C**H$_2$−O), 46.6, 43.0 (d, **C**H$_2$−N), 36.0 (s, **C**H$_2$−**C**H).

PAP (4b). Isolated yield: 63%. ^{1}H NMR (400 MHz, $CDCl_3$): δ 8.02−7.83 (m, Ar**H**), 7.59−7.46 (m, Ar**H**), 7.42−7.31 (m, Ar**H**), 5.25−5.09 (m, C**H**), 4.18−2.98 (m, C**H**$_2$), 2.98−2.13 (m, C**H**), 2.13−0.76 (m, C**H**$_2$). ^{13}C{^{1}H} CPMAS NMR (75 MHz): δ 173.2 (s, N−**C**═O), 46.9, 43.3 (d, **C**H$_2$−N), 35.8 (s, **C**H$_2$−**C**H), 26.2 (s, **C**H$_2$).

PAH (4c). Isolated yield: 83%. ^{1}H NMR (400 MHz, $CDCl_3$): δ 8.04−7.83 (m, Ar**H**), 7.60−7.17 (m, Ar**H**), 5.35−5.26 (m, C**H**), 3.92−2.96 (m, C**H**$_2$), 2.87−2.36 (m, C**H**), 2.21−1.01 (m, C**H**$_2$). ^{13}C{^{1}H} CPMAS NMR (75 MHz): δ 174.4 (s, N−**C**═O), 48.6 (d, **C**H$_2$−N), 37.1 (s, **C**H$_2$−**C**H), 27.4 (s, **C**H$_2$).

2.3.4. Diblock Copolymers I. Poly[(*N*-acryloylmorpholine)-*block*-(*N*-acryloylpiperidine)] (PAM-PAP, 5a) and Poly[(*N*-acryloylmorpholine)-*block*-(*N*-acryloylazocane)] (PAM-PAH, 5b) (Scheme 3). Series of PAM-PAP and PAM-PAH diblock copolymers were synthesized with [monomer]/[PAM] of 20, 50, 100, and 200 respectively. As an example, to add 50 units of PAP block to PAM ($\overline{M}_{n(NMR)}$ = 8330 Da), PAM macro CTA (0.12 mmol, 1 g), AP (6 mmol, 0.84 g), and AIBN (0.012 mmol, 2.0 mg) were mixed in dioxane (6.4 mL). All reaction conditions were identical with homopolymerization. In all cases, [PAM]/[AIBN] was maintained constant at 10.[46] Copolymers were precipitated in *n*-hexane and dried *in vacuo*. Average isolated yield was 77%.

2.3.5. *S*-[Poly(ethylene glycol) methoxy]carbonylphenylmethyl Dithiobenzoate (PEG-CTA). The synthesis of macro PEG RAFT agent (PEG-CTA) was adapted from that reported by Perrier et al.[64] with some modifications. All reactions were done under argon. PEG monomethyl ether (3.6 mmol, 7.2 g) was dissolved in toluene and dried by azeotropic distillation using a Dean−Stark trap. The residue was redissolved in THF (250 mL) by warming in a water bath and TEA (18.0 mmol, 2.5 mL) was added. CPAC (18.0 mmol, 3.6 mL) was added to the clear solution and the mixture stirred for 2 d at room temperature. The solution was concentrated under reduced pressure and the residue was dissolved in CH_2Cl_2 (150 mL). The clear solution was washed with $NaHCO_3$ (aq, 5% (w/v),

Scheme 4. Diblock Copolymerization II: Poly[(ethylene glycol)-*block*-(*N*-acryloylpiperidine)] (PEG-PAP, 6)

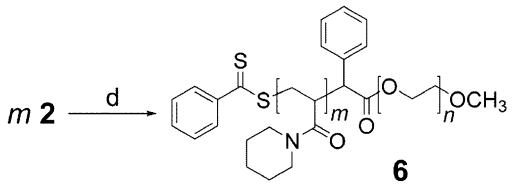

3 × 150 mL) and dried over Na_2SO_4. The mixture was filtered and PEG-CPAC recovered by precipitation in cold ether (100% conversion, confirmed by ^{1}H NMR). PEG-CPAC (3.2 g) was dissolved in THF (100 mL) and degassed under argon. phenylmagnesium chloride solution (2.0 M in THF, 3 mL) and carbon disulfide (2 mL) was mixed in an ice bath and added to the PEG-CPAC solution by a two-head needle connected through septa. The solution was refluxed overnight and a white solid formed during cooling was removed by filtration. PEG-CTA was washed with 1.0 M $KHSO_4$ (aq, 3 × 150 mL) and precipitated in cold diethyl ether (100% conversion, confirmed by ^{1}H NMR).

PEG-CPAC. Isolated yield: 87%. ^{1}H NMR (400 MHz, $CDCl_3$): δ 7.55−7.47 (m, Ar**H**), 7.42−7.33 (m, Ar**H**), 5.41−5.38 (s, C**H**), 4.40−4.25 (m, C**H**$_2$), 3.84−3.44 (s, OC**H**$_2$C**H**$_2$), 3.40−3.36 (s, C**H**$_3$).

PEG-CTA. Isolated yield: 59%. ^{1}H NMR (400 MHz, $CDCl_3$): δ 8.06−7.92 (d, Ar**H**), 7.60−7.32 (m, Ar**H**), 5.78−5.66 (s, C**H**), 4.44−4.22 (m, C**H**$_2$), 3.84−3.42 (s, OC**H**$_2$C**H**$_2$), 3.40−3.34 (s, C**H**$_3$).

2.3.6. Diblock Copolymers II. Poly[(ethylene glycol)-*block*-(*N*-acryloylpiperidine)] (PEG-PAP, 6) (Scheme 4). PEG-PAP diblock copolymers were synthesized with [AP]/[PEG-CTA] of 20, 50, 100, and 200 respectively. As an example, to add 50 units of PAP block, PEG-CTA (0.121 mmol, 0.26 g), AP (6.1 mmol, 0.84 g), and AIBN (0.0121 mmol, 2.0 mg) were mixed in dioxane (4 mL). All reaction conditions were identical with homopolymerization. In all cases, [PEG-CTA]/[AIBN] was fixed constant at 10. Copolymers were recovered with 56% of isolated yield in average. Copolymers were precipitated in *n*-hexane and dried *in vacuo*.

2.4. Aggregate Formation. Adequate amount of polymers (10−80 mg) were dissolved in *N*-methyl-2-pyrrolidone (NMP) (0.5−1 mL), placed in regenerated cellulose membrane (MWCO 1 kDa or 10 kDa, Spectrum Laboratories, Breda, The Netherlands), and dialyzed against water (5 L) for 1−2 d by regularly replacing the water. Mean size of aggregates was determined using a Malvern Zetasizer Nano ZS equipped with He/Ne laser at 633 nm. All values are given as volume-average hydrodynamic diameter.

2.5. Cmc Determination. The cmcs of the block copolymers were determined by the fluorescence probe technique with pyrene.[65] Aqueous polymer solution (500 μL) was sequentially diluted and mixed with pyrene solution (1 μL, 1×10^{-3} M in absolute ethanol). The final concentration of pyrene was adjusted to 2×10^{-6} M. Each solution (200 μL) was transferred to 96-well microplate. In 30−40 min, I_1/I_3 was determined with a microplate reader, from $\lambda_{em} = 377$ nm (I_1) and 386 nm for (I_3) with $\lambda_{ex} = 355$ nm. To determine the cmc, the I_1/I_3 ratio was plotted vs polymer concentration in a semilogarithmic scale. The plotted points were fitted according to the eq 1 by using Origin software (v. 7.03). We regarded the inflection points of the fitted curve as the cmcs. Thus, the inflection point was determined as the minimum of the derivative of the fitted curve obtained from eq 1

$$y = A_2 + \frac{A_1 - A_2}{1 + e^{x - x_0/dx}} \quad (1)$$

where $x = \log(C)$, $y = I_1/I_3$. C is the molarity of polymer. Constants x_0, A_1, and A_2 denote the center, the initial value, and the final value respectively.

2.6. TEM. Aggregates suspension in water (5 μL, 1−5% (w/v)) was placed on the carbon-coated grid (400 mesh) for 1 min, and the grid was washed with distilled water. For the negative staining, the grid was treated with uranyl acetate aqueous solution (5 μL, 2% (w/v)) for 30 s and the excess solution was blotted away to a filter paper. Samples were observed with Philips CM12 operated at 80 kV.

2.7. *in vitro* Release of Everolimus from PAM-PAH Micelles. Everolimus (2 mg, $\lambda_{max} = 278$ nm) was dissolved in acetone (200 μL) and then slowly added to 1 mL of PAM(0.15)-PAH(0.85) micelle suspension (10 mg/mL). The solution was stirred overnight to allow all residual acetone to be evaporated and centrifuged with a speed of 13 000 rpm for 10 min to sediment unloaded drug. The supernatant was carefully taken and the total volume was adjusted at 2 mL by adding PBS (pH 7.4, 10 mM). The solution was placed into upper part of centrifugal filter device (Amicon Ultra-MWCO 5000 Da, Millipore, Carrigtwohill, Ireland). The lower part was filled with PBS (pH 7.4, 10 mM), which was frequently replaced with fresh solution. The whole solution was incubated at 37 °C with 5% CO_2 supply. A known amount of the upper solution (100 μL) was taken at predetermined time points, lyophilized, and redissolved in the same volume of THF (100 μL). The withdrawn solution (20 μL) was injected into a SEC module (eluent: THF, flow rate: 1 mL/min, temperature: 40 °C) and the absorbance at 278 nm was monitored with Waters 996 PDA. The loaded amount of everolimus was calculated based on a calibration curve ($R^2 = 0.9999$) obtained from already-known concentrations of everolimus/THF solutions. From the amount of remaining everolimus, the released amount of drug was inversely calculated by subtracting the amount of remaining drug from the amount of loaded drug calculated at zero time point.

3. Results and Discussion

3.1. Monomer Synthesis: AM, AP, and AH. The scheme for AM synthesis and AP synthesis has been already reported,[61,63,66] yet to our limited knowledge, the acylation of azocane is first reported here. Three monomers (AM, AP, AH) were synthesized by nucleophilic substitution of secondary cyclic amines with acryloyl chloride as shown in Scheme 1. Monomers were successively washed with mild acid to remove basic salt and with base to remove hydrolyzed acid adduct from acryloyl chloride. The yields for AP and AH were higher than AM, consistent with higher hydrophilicity of AM than AP and AH. ^{1}H NMR and mass spectrometry confirmed the structures accordingly. (See Figures S1a−c in the Supporting Information for ^{1}H NMR spectra of all monomers.)

3.2. Homopolymerization: PAM, PAP, and PAH. The selection of the CTA is very critical in designing RAFT polymerization. Since there is no clear-cut rule in selecting an optimal CTA, intensive studies have been devoted to finding an adequate CTA for various specific systems. As for PAM, Fabier et al. exploited different species of CTAs such as *tert*-butyl dithiobenzoate, carboxymethyl dithiobenzoate, (1-(4-methylcyclohexan-2-onyl)-1-methyl)ethyl dithiobenzoate (menthonyl dithiobenzoate), 1,3-bis(2-(thiobenzoylthio)prop-2-yl)benzene.[46,48] In addition, D'agosto et al. reported that a CTA with a phenyl group at the *Z* position (stabilizing group) with β-propionic acid for the *R* position (good leaving group) exhibits better performance over benzyl dithioestyl group at the *Z* position.[45] On the basis of these pioneering works, we selected 2-[(2-phenyl-1-thioxo)thio]propanoic acid, hereafter referred to simply as CTA. Thus, in this work, by synthesizing all homopolymers under the same conditions—temperature, solvent, CTA, [monomer]/[CTA], etc.—we examined our hypothesis that AP and AH would behave the same as AM in RAFT polymerization.

First, the CTA was well synthesized as characterized by TLC and ^{1}H NMR with a slightly higher yield than previously

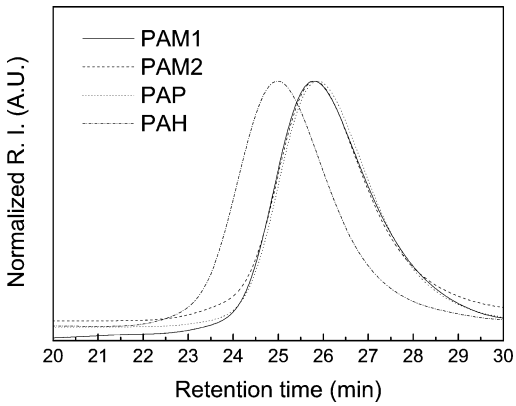

Figure 1. Size exclusion chromatograms in overlay for homopolymers; poly(*N*-acryloylmorpholine) (PAM), poly(*N*-acryloylpiperidine) (PAP), and poly(*N*-acryloylazocane) (PAH). THF was used as an eluent at 1 mL/min of flow rate and 40 °C.

reported. (See Figure S1d in the Supporting Information for the ^{1}H NMR spectrum of CTA.) We note that it is worthwhile to mention here that the distillation step in CTA synthesis is critical, as distillation is the only way to remove residual 2-bromopropionic acid and obtain a clean product. Several other methods were attempted (i.e., extraction, recrystallization, etc.), yet no other method was successful. Careful heating of the distillation apparatus' connections, where the heat could be lost, was required to achieve higher yield. After obtaining CTA, homopolymerizations were done under the conditions as described in the Experimental Section. All homopolymers were targeted to consist of 50 monomeric units. As can be seen in Figure 1, all three homopolymers were obtained with a monomodal distribution. The targeted number-average molecular weight ($\overline{M}_{n(theor)}$) was calculated based on eqs 2 and 3 as follows,[46]

$$\overline{M}_{n(theor)} = \frac{[A]_0 \times M_{AM} \times N_{theor}}{[CTA]_0 + 2f[AIBN]_0(1 - e^{-k_d t})(1 - f_c/2)} + M_{CTA} \quad (2)$$

$$\overline{M}_{n(theor)} \cong \frac{[A]_0 \times M_{AM} \times N_{theor}}{[CTA]_0} + M_{CTA} \quad (3)$$

where N_{theor} is the targeted degree of polymerization, $[A]_0$ is the initial concentration of monomer, $[AIBN]_0$ is the initial concentration of AIBN, $[CTA]_0$ is the initial concentration of CTA, f is the efficiency factor of AIBN, k_d is the decomposition rate constant for AIBN, f_c is the percentage of coupling reactions relatively to the overall termination reactions, M is the molecular weight, and t is the duration of polymerization.

The number-average molecular weights ($\overline{M}_n$) of homopolymers were determined by different methods. The results are summarized in Table 1. To calculate $\overline{M}_{n(theor)}$, we simplified eq 2 to eq 3 under a more practical assumption that (1) the reaction goes to the completion and (2) the concentration of AIBN was negligibly smaller than other reagents such as CTA or monomer. From the ^{1}H NMR spectra for PAM, PAP, and PAH, three separate peaks (8.0−7.3 ppm) for the five protons of the phenyl ring of the phenyl dithioester were clearly resolved in a 2:1:2 integral ratio. By comparing the integral values of these protons with those of the protons on the aliphatic rings and polyacrylamide backbones (4.1−0.9 ppm), $\overline{M}_{n(NMR)}$ was correspondingly calculated and were in a reasonable agreement with $\overline{M}_{n(theor)}$. (See Figure S2 in the Supporting Information for ^{1}H NMR spectra of PAM, PAP, and PAH.) As an alternative method, $\overline{M}_{n(UV/vis)}$ was calculated from the optical absorbance of the phenyl dithioester groups at 496 nm. Sequentially diluted CTA solutions in DMSO (PAM, PAP) or MeOH (PAH) were used to create a calibration curve to which the optical density of the known concentration of polymer solution in the same solvent was correlated. The results deviated slightly from $\overline{M}_{n(NMR)}$, yet were still acceptable.

In order to record ^{13}C{1H} CPMAS NMR spectra of solid PAM, PAP, and PAH homopolymers, the cross-polarization (CP) technique is used to transfer the magnetization from protons to carbons under magic angle spinning (MAS). This is done to increase the signal intensity and to collect data more rapidly as the spin−lattice relaxations of protons are often much longer than those of carbons. Because of high crystallinity and impressive polydispersity, all ^{13}C resonances are just moderately broad. For all homopolymers, ^{13}C signals of the amide carbonyl groups (C3) appear between 173 and 175 ppm while backbone carbons (C1 and C2) commonly result in signals between 36 and 37 ppm. The spectrum of PAM displays a characteristic peak at 67 ppm, which is attributed to the carbon atoms (C6 and C7) adjacent to the oxygen atom while in other homopolymers they are observed between 26 and 28 ppm as expected. Furthermore, carbons adjacent to nitrogen (C4 and C5) of PAM and PAP result in two nicely resolved resonances as a consequence of their nonequivalent chemical environment due to rigid amide bond. In spectra of PAH, they are not resolved possibly due to larger line widths and smaller chemical shift separation. Signals of the phenyl dithioester groups and 2-propionic acid groups from the RAFT agent are not visible. (See Figure S3 in the Supporting Information for ^{13}C{^{1}H} CPMAS NMR spectra for homopolymers.)

3.3. Copolymerization I: PAM-PAP and PAM-PAH. As discussed above, PAM still possesses the phenyl dithioester groups and thus can be used as a macromolecular CTA (macro CTA) in diblock copolymerization with AP and AH. Reaction conditions were the same as for homopolymerization. Two different batches of PAM (PAM1 and PAM2) were used to copolymerize with AP for PAM-PAP series and AH for PAM-PAH series, respectively.

From the ^{1}H NMR spectra of a series of PAM-PAP copolymers, three characteristic regions, namely 4.1−2.9 ppm (region A), 2.9−2.1 ppm (region B), 2.1−1.0 ppm (region C), were evolved as longer PAP blocks were added to PAM. Phenyl dithioester groups were still observed at the same position. However, the molecular weight calculated from phenyl dithioester end groups differed from the theoretically estimated molecular weight. This discrepancy may partially stem from destroyed end groups, for example, by oxidation of the dithioester into sulfine and/or thioester and/or sulfide species, etc.[47] because the end groups on the macro CTA are exposed to oxygen or other oxygen-containing solvents during a second round of polymerization and excessive purification steps. It can also be hypothesized that the end groups become more diluted, as polymer chains grow larger, leading to a signal broadening effect and less-defined integral values. For this reason, since $\overline{M}_{n(NMR)}$ could not be accurately determined in the same way as with the homopolymers, we decided to calculate $\overline{M}_{n(NMR)}$ by comparing the integral values of three separable regions: region A, region B, and region C. In the same way, $\overline{M}_{n(NMR)}$ of PAM-PAH was also calculated.

The integral values for region A and C are both contributed by the protons on the aliphatic rings of PAM and PAP/PAH plus two protons of polyacrylamide backbone. The coefficients in eqs 4 and 5 were derived from the theoretical integral values

Table 1. Characterization of Homopolymers[a,b]

	$\overline{M}_{n(theor)}$	$\overline{M}_{n(NMR)}$	$\overline{M}_{n(UV/vis)}$	$\overline{M}_{w(SEC)}$	$\overline{M}_{n(SEC)}$	PD[c]
PAM1	7280	8330	6600	8110	7840	1.02[d]
PAM2	7280	6480	7210	7770	6590	1.18[e]
PAP	7190	7100	6500	6780	6630	1.03[d]
PAH	8590	8350	7020	9750	7960	1.22[e]

[a] All molecular weights are given in Da. [b] Abbreviations for polymers: poly(*N*-acryloylmorpholine) (PAM), poly(*N*-acryloylpiperidine) (PAP), poly(*N*-acryloylazocane) (PAH). [c] Polydispersity. [d] Determined from THF-eluting SEC module. [e] Determined from DMF-eluting SEC module.

Table 2. Characterization of Diblock Copolymers-I[a,b,c]

	$\overline{M}_{n(theor)}$	$\overline{M}_{n(NMR)}$	$\overline{M}_{n(EO/AM,NMR)}$	$\overline{M}_{n(AP/AH,NMR)}$	$\overline{M}_{w(SEC)}$	$\overline{Mn}_{(SEC)}$	PD[d]
PEG(0.47)-PAP(0.53)	5010	4710	2230	2480	3780	3040	1.24
PEG(0.41)-PAP(0.59)	9600	7210	2230	4980	7150	5910	1.21
PEG(0.16)-PAP(0.84)	16 200	14 200	2230	12 000	9920	8000	1.24
PEG(0.09)-PAP(0.91)	30 100	24 100	2230	21 900	20 600	17 100	1.20
PAM(0.66)-PAP(0.34)	14 800	12 300	8100	4120	7680	6450	1.19
PAM(0.54)-PAP(0.46)	16 900	14 900	8100	6830	9970	8350	1.19
PAM(0.43)-PAP(0.57)	22 000	18 800	8100	10 700	11 600	11 100	1.05
PAM(0.24)-PAP(0.76)	35 900	33 200	8100	25 100	20 900	17 400	1.20
PAM(0.63)-PAH(0.37)	9210	9930	6250	3680	9790	8060	1.21
PAM(0.43)-PAH(0.57)	13 600	14 400	6250	8180	13 600	11 000	1.24
PAM(0.26)-PAH(0.74)	21 000	24 100	6250	17 900	22 400	18 100	1.24
PAM(0.15)-PAH(0.85)	35 800	41 400	6250	35 100	30 800	23 400	1.32

[a] All molecular weights are given in Da. [b] As Relogio et al. indicated in ref 52, size exclusion chromatography (SEC) is not highly recommended to determine the molecular weight of copolymers. Thus, we anticipate the presented results are qualitatively regarded. [c] Abbreviations for polymers: poly[(ethylene glycol)-*block*-(*N*-acryloylpiperidine)] (PEG-PAP), poly[(*N*-acryloylmorpholine)-*block*-(*N*-acryloylpiperidine)] (PAM-PAP), poly[(*N*-acryloylmorpholine)-*block*-(*N*-acryloylazocane)] (PAM-PAH), where the numbers in parentheses denote the weight fraction of each block. [d] Polydispersities determined from DMF-eluting SEC module, where PD denotes polydispersity.

of ^{1}H NMR spectra of the homopolymers (PAM, PAP, PAH). By normalizing the integral value of region A and C to region B, by setting it to unity, the molar fraction of AM, AP, or AH (X_{AM}, X_{AP} or X_{AH}) can be calculated. The molecular weights of end groups were not considered for the calculation of weight fraction of both blocks.

$$8 \times X_{AM} + 4 \times X_{AP} = I_A \quad 2 \times X_{AM} + 8 \times X_{AP} = I_C \qquad (4)$$

$$8 \times X_{AM} + 4 \times X_{AH} = I_A \quad 8 \times X_{AM} + 12 \times X_{AH} = I_C \qquad (5)$$

where $X_{AM} = N_{AM}/N_t$, $X_{AP} = N_{AP}/N_t$, $X_{AH} = N_{AH}/N_t$, and $N_t = N_{AM} + N_{AP}$ or $N_t = N_{AM} + N_{AH}$, I_A is the integral value of region A, and I_C is the integral value of region C, with $N_{AM} =$ 57.4 and 44.3 for PAM1 and PAM2 respectively. (See Figure S4, parts a and b in the Supporting Information for the ^{1}H NMR spectra of PAM-PAP and PAM-PAH series.)

As given in Table 2, monomodal distribution was still maintained. Importantly, the molecular weight evolution of copolymers is clearly seen by the shift of retention time as the molecular weights of the second block increase (see Figure 2 for size exclusion chromatograms in overlay of PAM-PAP series and Figure S5a for size exclusion chromatograms in overlay of PAM-PAH series in the Supporting Information). Narrowly resolved spectra indicate well-controlled copolymerization with the PAM macro CTA. Our results are slightly different from those reported in a previous study, in which the copolymerization of PAM with styrene was attempted, yet multimodal distribution was achieved.[45] This suggests that the difference in polymerizing character of monomers is very crucial to the design of the block copolymerization from living polymeric CTA under the constant conditions.

3.4. Copolymerization II: PEG-PAP. To study the effect on aggregation behavior of PAM as a hydrophilic block, we also prepared a block copolymer composed of PEG and PAP. There have been several reports concerning how to incorporate PEG in block copolymers via RAFT polymerization.[64,67,68] In this work, PEG-derived macro CTA (PEG-CTA) was synthesized in two steps from PEG monomethoxy ether as reported by Perrier et al.[64] We found that the azeotropic distillation of the starting PEG is crucial to prepare PEG-CTA. When this step was omitted, PEG-CPAC was poorly functionalized with low conversion rate (18−37%) as determined from ^{1}H NMR spectra. This may be due to the partial hydrolysis of CPAC groups into acids caused by water hydration, which leads to a lesser degree of functionalization. Thus, before PEG was subjected to the reaction with CPAC, the azeotropic distillation was done in toluene, although it is not described in the original literature. It is also important to note that the diethyl ether precipitation after the second step should be executed very carefully to remove colored impurities. PEG-CTA thus synthesized showed complete functionalization as confirmed by ^{1}H NMR. In addition, as evident from SEC monomodality, no structural change such as coupling or degradation occurred during the reaction (data not shown).

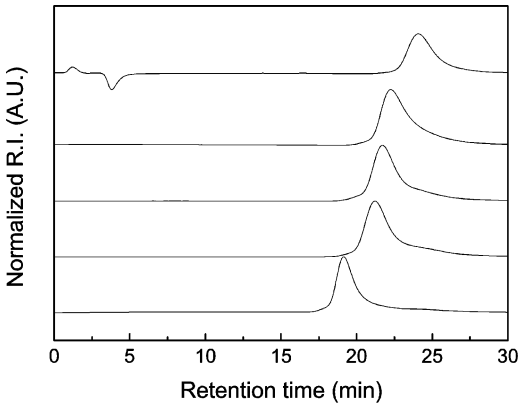

Figure 2. Size exclusion chromatograms in overlay for diblock copolymers; poly(*N*-acryloylmorpholine) (PAM) macro CTA and various poly[(*N*-acryloylmorpholine)-*block*-(*N*-acryloylpiperidine)] diblock copolymers abbreviated as PAM(0.66)-PAP(0.34), PAM(0.54)-PAP-(0.46), PAM(0.43)-PAP(0.57), and PAM(0.24)-PAP(0.76) (from top). The numbers in parentheses denote the weight fraction of each block. THF was used as an eluent at 1 mL/min of flow rate and 40 °C.

Table 3. Solubility of Homopolymers in Various Solvents at Room Temperature[a,b]

	polarity index[70]	PEG	PAM	PAP	PAH
water	9.0	soluble	soluble	insoluble	insoluble
formamide	7.3	soluble	soluble	soluble	insoluble
nitromethane	6.8	soluble	soluble	soluble	insoluble
methanol	6.6	soluble	swollen	soluble	soluble
DMSO	6.5	soluble	soluble	soluble	insoluble
NMP	6.5	soluble	soluble	soluble	soluble
DMF	6.4	soluble	soluble	soluble	soluble
DMAc	6.3	soluble	soluble	soluble	soluble
acetonitrile	6.2	soluble	soluble	soluble	insoluble
acetone	5.4	soluble	soluble	soluble	swollen
ethanol	5.2	soluble	insoluble	soluble	soluble
1,4-dioxane	4.8	soluble	soluble	soluble	soluble
chloroform	4.4	soluble	soluble	soluble	soluble
iso-propanol	4.3	insoluble	insoluble	soluble	soluble
ethyl acetate	4.3	soluble	insoluble	soluble	soluble
THF	4.2	soluble	soluble	soluble	soluble
DCM	3.4	soluble	soluble	soluble	soluble
toluene	2.3	soluble	soluble	soluble	soluble
n-hexane	0.0	insoluble	insoluble	insoluble	insoluble

[a] Abbreviations for solvents: dichloromethane (DCM), *N*,*N*-dimethylacetamide (DMAc), *N*,*N*-dimethylformamide (DMF), dimethylsulfoxide (DMSO), *N*-methyl-2-pyrrolidone (NMP), tetrahydrofuran (THF). [b] Abbreviations for polymers: poly(ethylene glycol) (PEG), poly(*N*-acryloylmorpholine) (PAM), poly(*N*-acryloylpiperidine) (PAP), poly(*N*-acryloylazocane) (PAH).

PEG-CTA was further polymerized with AP under the same conditions as for PAM homopolymerization. The degree of polymerization was calculated by comparing the average of the integral values of region B (2.9−2.1 ppm) and region C (2.1−1.0 ppm) to the integral value of region A (4.1−2.9 ppm) subtracted from the known integral value for the given molecular weight of PEG (at ∼3.5 ppm). The results calculated are listed in Table 2. After copolymerization, ^{1}H NMR spectra showed no evidence of hydrolysis of the ester between PEG and PAP, as no COOH groups or OH groups could be detected in ^{1}H NMR spectra with either DMSO-d_6 or $CDCl_3$. (^{1}H NMR spectra with DMSO-d_6 are not shown. See Figure S4c in the Supporting Information for ^{1}H NMR spectra with $CDCl_3$ for the PEG-PAP series.) Size exclusion chromatograms also confirmed that single peaks were mostly resolved, demonstrating that copolymerization was successful on all PEG-CTA chains. (See Figure S5b in the Supporting Information for size exclusion chromatograms in overlay of the PEG-PAP series.)

3.5. Aggregate Formation.

3.5.1. Solubility. The solubility of all homopolymers, namely PEG, PAM, PAP, and PAH, was tested with different solvents as listed in Table 3. A total of 19 different solvents were chosen with different polarities, from water (maximum polarity) to *n*-hexane (minimum polarity). As expected, PAM was completely soluble in water, but remained insoluble in aliphatic alcohols such as ethanol and iso-propanol. PAM was insoluble in ethyl acetate and *n*-hexane as well. Notably, a discrepancy was found in the solubility of PAM with 1,4-dioxane and methanol from the previous studies.[43,69]

For instance, from our experiments, PAM was not completely soluble in methanol, but slightly swollen. In contrast, PAM was completely soluble in 1,4-dioxane. This discrepancy may arise from different molecular weight or difference in polymer architecture (i.e., linear or partially branched), because earlier studies dealt with PAM synthesized by free radical polymerization. As previously known, PAP was insoluble in water at room temperature. However, when it was cooled to below 4 °C, the solution turned transparent and by warming to the ambient temperature, it reversibly regained its turbidity. These observations are ascribed to the reported LCST (4−6 °C) for PAP.[61,71] PAP was soluble in all organic solvents used in this study except *n*-hexane. PAH, which to our knowledge has not been previously reported, behaves quite differently from PAM and PAP. PAH was poorly soluble in polar solvents such as formamide, nitromethane, acetonitrile, and DMSO. In acetone, PAH was not dissolved well, but remained in a swollen state. As expected, PAH was not soluble in water. Differently from PAP, PAH did not undergo any phase transition to 0 °C. PEG was soluble in most solvents except *n*-hexane and 2-propanol.

3.5.2. Selection of a Cosolvent. Dialysis is a common technique to form aggregates from amphiphilic block copolymers. The polymer is dissolved in a cosolvent which dissolves both hydrophilic and hydrophobic segments and the solution is dialyzed against water to induce slow solvent exchange. As the solvent diffuses through the dialysis membrane, the hydrophobic segments come into contact with the aqueous phase and start to aggregate to form self-assembled structures in a specific topology. For this reason, to form aggregates by dialysis, one should find a cosolvent that (1) is capable of dissolving each block commonly and (2) is miscible with water to facilitate solvent exchange. NMP, DMF, DMAc, 1,4-dioxane, and THF fulfilled these prerequisites. However, except for NMP, all solvents led to polymer gelation or agglomeration during dialysis. Since it is known that the cosolvent itself can affect the size and morphology of aggregates,[72] NMP was used as a cosolvent for all experiments in this study.

3.5.3. Particle Size and Morphology Analyses by DLS and TEM. Table 4 shows the degrees of polymerization for the hydrophilic block ($N_{EO/AM}$), hydrophobic block ($N_{AP/AH}$), and the overall degree of polymerization (N_t) for the copolymers examined. The molecular weight of the end group is not taken into account, assuming that end groups do not influence the aggregation behavior. Since the densities of the homopolymers are not known, the weight fraction (w) was used instead of the volume fraction. Thus, if one assumes the densities of all polymers are close to 1 g/mL, volume fractions will not greatly differ from the weight fractions. For more comprehensive notation, hereafter the weight fractions of each block are shown in parentheses next to each block.

The mean hydrodynamic diameters (D) of the polymers as measured by DLS are given in Table 5, and Figure 3a-c show D as a function of the aggregation number Z (listed in Table 5), $w_{AP/AH}$, and $\chi_{AP/AH}$. All series of copolymers except for PEG(0.09)-PAP(0.91) behaved quite similarly, with a linear relation of D and Z as a function of $w_{AP/AH}$ and/or $\chi_{AP/AH}$. This means that the substitution of PAM by PEG did not result in any dramatic change in the size of aggregates up to $w_{AP/AH} = 0.85$. With similar $w_{AP/AH}$ values, PEG(0.16)-PAP(0.84), PAM(0.24)-PAP(0.76), and PAM(0.26)-PAH(0.74) formed aggregates with similar D: 35, 33, and 33 nm, respectively. One notes that the PEG(0.09)-PAP(0.91) copolymer does not fit the trend; it is different from other PEG-PAP copolymers, with lower $w_{AP/AH}$ values. Thus, we examined the morphologies of some aggregates formed from PEG(0.09)-PAP(0.91), PAM(0.24)-PAP(0.76), and PAM(0.15)-PAH(0.85) with TEM.

As shown in Figure 4, the morphologies of the aggregates from PAM (0.24)-PAP(0.76) and PAM(0.15)-PAH(0.85) were commonly found as spherical micelles, while PEG(0.09)-PAP(0.91) formed a mixture of spherical micelles and larger spherical aggregates. Interestingly, from the histogram of particle size analysis (data not shown), PEG(0.09)-PAP(0.91) showed bimodal distribution with significantly larger size and standard deviation than two others, which were in a narrow and

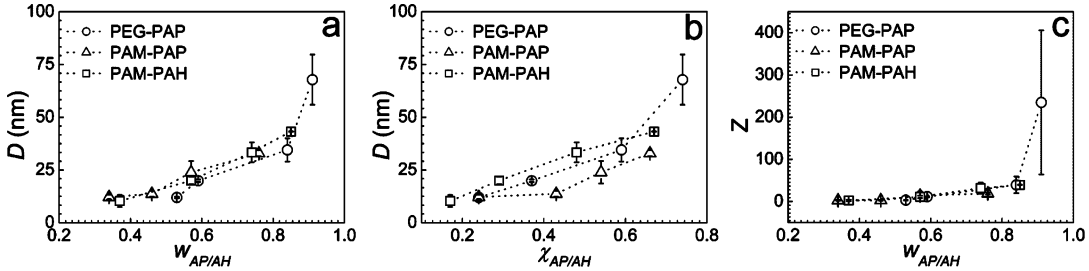

Figure 3. Plots for the aggregates with a) D vs $w_{AP/AH}$, (b) D vs $\chi_{AP/AH}$, and (c) Z vs $w_{AP/AH}$. (error bar: SD for $n = 3$) Abbreviations for diblock copolymers: poly[(ethylene glycol)-*block*-(*N*-acryloylpiperidine)] (PEG-PAP), poly[(*N*-acryloylmorpholine)-*block*-(*N*-acryloylpiperidine)] (PAM-PAP), and poly[(*N*-acryloylmorpholine)-*block*-(*N*-acryloylazocane)] (PAM-PAH), where the numbers in parentheses denote the weight fraction of each block. χ indicates the fraction of the degree of polymerization ($\chi_{AP/AH} = N_{AP/AH}/N_t$, where $N_t = N_{EO/AM} + N_{AP/AH}$) and w indicates the weight fraction and Z indicates the aggregation number.

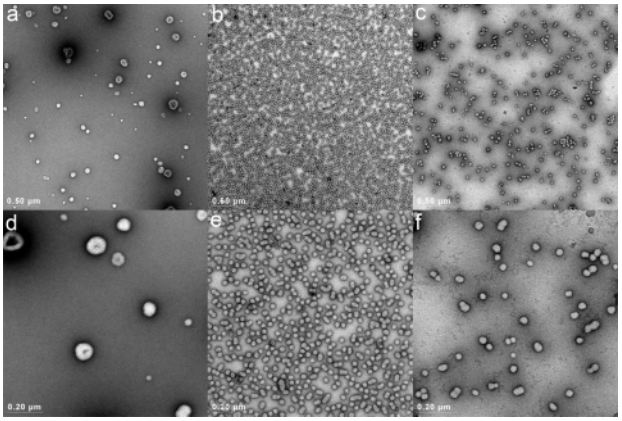

Figure 4. TEM images of the aggregates from PEG(0.09)-PAP(0.91) (a and d), PAM(0.24)-PAP(0.76) (b and e), and PAM(0.15)-PAH(0.85) (c and f), where PEG-PAP denotes poly[(ethylene glycol)-*block*-(*N*-acryloylpiperidine)] and PAM-PAP denotes poly[(*N*-acryloylmorpholine)-*block*-(*N*-acryloylpiperidine)] and PAM-PAH denotes poly[(*N*-acryloylmorpholine)-*block*-(*N*-acryloylazocane)]. The numbers in parentheses denote the weight fraction of each block. All samples were negatively stained with 2% (aq, w/v) uranyl acetate solution.

Table 4. Characterization of Diblock Copolymers II[a,b,c]

	$N_{EO/AM}$	$N_{AP/AH}$	N_t	$\chi_{AP/AH}$[d]	$w_{AP/AH}$[d]
PEG(0.47)-PAP(0.53)	50.7	17.8	68.5	0.24	0.53
PEG(0.41)-PAP(0.59)	50.7	35.8	86.5	0.37	0.59
PEG(0.16)-PAP(0.84)	50.7	85.9	137	0.59	0.84
PEG(0.09)-PAP(0.91)	50.7	157	208	0.74	0.91
PAM(0.66)-PAP(0.34)	57.4	29.6	87.0	0.24	0.34
PAM(0.54)-PAP(0.46)	57.4	49.1	107	0.43	0.46
PAM(0.43)-PAP(0.57)	57.4	76.6	134	0.54	0.57
PAM(0.24)-PAP(0.76)	57.4	180	238	0.66	0.76
PAM(0.63)-PAH(0.37)	44.3	22.0	66.3	0.17	0.37
PAM(0.43)-PAH(0.57)	44.3	48.9	93.2	0.29	0.57
PAM(0.26)-PAH(0.74)	44.3	107	152	0.48	0.74
PAM(0.15)-PAH(0.85)	44.3	210	254	0.67	0.85

[a] Subscript, EO/AM denotes the hydrophilic block (PEG or PAM) and AP/AH denotes the hydrophobic block (PAP or PAH). [b] N denotes the degree of polymerization. [c] Abbreviations for diblock copolymers: poly[(ethylene glycol)-*block*-(*N*-acryloylpiperidine)] (PEG-PAP), poly[(*N*-acryloylmorpholine)-*block*-(*N*-acryloylpiperidine)] (PAM-PAP), poly[(*N*-acryloylmorpholine)-*block*-(*N*-acryloylazocane)] (PAM-PAH), where the numbers in parentheses denote the weight fraction of each block. [d] χ indicates the fraction of degree of polymerization ($\chi_{AP/AH} = N_{AP/AH}/N_t$), where $N_t = N_{EO/AM} + N_{AP/AH}$ and w indicates the weight fraction.

monomodal distribution of particle size. As for PEG(0.09)-PAP(0.91), notably, wormlike micelles were not observed as a continuum from spherical micelles to polymersomes. Although it is not clear from the negatively stained TEM images, three possibilities may be hypothesized: (1) the larger objects may not represent equilibrium structure, (2) an identical morphology, "crew-cut" micelles or bilayer polymersomes may be in different size, and (3) two different morphologies, spherical micelles and bilayer polymersomes, may coexist. However, besides the morphology of the aggregates, the sizes measured from TEM images correlated well with the results obtained by DLS measurement: 68 ± 12 nm (DLS), 57 ± 19 nm (TEM) for PEG(0.09)-PAP(0.91); 33 ± 1.4 nm (DLS), 35 ± 4.1 nm (TEM) for PAM(0.24)-PAP(0.76); 43 ± 0.1 nm (DLS), 41 ± 6.6 nm (TEM) for PAM(0.15)-PAH(0.85).

3.5.4. Cmc Determination. To better characterize aggregate formation, the cmc was determined for all block copolymers. There are many methods to determine cmc, such as fluorescence micellization,[65,73,74] dye solubilization,[75−77] and surface tension measurement.[78,79] In this work, as described in the Experimental Section, we employed pyrene as a fluorescent probe, determining the cmc as the inflection point in the fit of the I_1/I_3 ratio plotted vs polymer concentration in a semilogarithmic scale as seen in Figure 5a-c.

For all polymers, cmcs were in the range from 1×10^{-2} to 5×10^{-7} M, as listed in Table 5. With an identical length of hydrophile, cmc values decreased with increasing molecular weight of hydrophobes, as is typically observed for amphiphilic block copolymers. Except for PAM(0.24)-PAP(0.76) and PAM-(0.15)-PAH(0.85), all polymers obeyed the linear inverse correlation in a semilogarithmic plot (Figure 5d). This agrees well as reported for low molecular weight amphiphiles.[79] Thus, the results clearly support that all of the examined block copolymers formed aggregates.

3.5.5. Segregation Behavior. Extending the discussion from the previous section, two important characterization parameters were further considered, namely δ, the segregation factor, and Z. First, segregation factors were calculated from the overall degree of polymerization (N_t) and hydrodynamic radius (R) as obtained from DLS. Z values, presented in Table 5 as well, denote the number of copolymer chains per aggregate. Forster et al. has reviewed[80] three major segregation models: the weak segregation model and the strong segregation model as studied by Bates and co-workers[81] and the super strong segregation model by Nyrkova et al.[82] On the basis of those studies, segregation factors can be calculated to give better insight into the segregating behavior of the block copolymers. While the entire group of the PAM-PAP series belonged to the weak segregation region (WSR), the PAM-PAH series, except for PAM(0.63)-PAH(0.37), fell into the strong segregation region (SSR) located between the strong segregation limit (SSL) and weak segregation limit (WSL). The PEG-PAP series was positioned very similarly with PAM-PAH except for PEG(0.09)-PAP(0.91), which reached SSL. However, due to the different morphology (polymersomes vs spherical micelles), PEG(0.09)-PAP(0.91) should not be directly compared to others.

Table 5. Characterization of Aggregates Formed from Diblock Copolymers with NMP as a Cosolvent[a,b]

	N_t	D (nm)	cmc (M)	δ^c	Z^d
PEG(0.47)-PAP(0.53)	68.5	12 ± 0.3	(1.02 ± 0.81) × 10^{-2}	0.424 ± 0.007	3.16 ± 0.28
PEG(0.41)-PAP(0.59)	86.5	20 ± 0.6	(5.90 ± 3.83) × 10^{-4}	0.515 ± 0.007	11.5 ± 1.06
PEG(0.16)-PAP(0.84)	137	35 ± 5.5	(1.42 ± 0.97) × 10^{-4}	0.577 ± 0.031	39.4 ± 19.7
PEG(0.09)-PAP(0.91)	208	68 ± 12	(7.56 ± 2.06) × 10^{-6}	0.664 ± 0.042	235 ± 171
PAM(0.66)-PAP(0.34)	87.0	12 ± 1.1	(1.33 ± 0.56) × 10^{-3}	0.404 ± 0.020	2.63 ± 0.67
PAM(0.54)-PAP(0.46)	107	14 ± 1.4	(3.61 ± 1.38) × 10^{-4}	0.411 ± 0.021	3.07 ± 0.97
PAM(0.43)-PAP(0.57)	134	24 ± 5.3	(3.84 ± 1.11) × 10^{-5}	0.504 ± 0.043	14.1 ± 9.81
PAM(0.24)-PAP(0.76)	238	33 ± 1.4	(5.16 ± 4.71) × 10^{-6}	0.512 ± 0.008	18.8 ± 2.34
PAM(0.63)-PAH(0.37)	66.3	10 ± 2.9	(1.54 ± 1.10) × 10^{-3}	0.382 ± 0.073	2.34 ± 1.57
PAM(0.43)-PAH(0.57)	93.2	20 ± 1.7	(6.87 ± 7.65) × 10^{-5}	0.508 ± 0.019	10.9 ± 2.79
PAM(0.26)-PAH(0.74)	152	33 ± 4.7	(1.53 ± 1.06) × 10^{-6}	0.559 ± 0.028	31.7 ± 13.2
PAM(0.15)-PAH(0.85)	254	43 ± 0.1	(4.62 ± 3.46) × 10^{-7}	0.555 ± 0.001	39.4 ± 0.42

[a] All values represent Mean ± SD for $n = 3$. [b] Abbreviations for diblock copolymers: poly[(ethylene glycol)-*block*-(*N*-acryloylpiperidine)] (PEG-PAP), poly[(*N*-acryloylmorpholine)-*block*-(*N*-acryloylpiperidine)] (PAM-PAP), poly[(*N*-acryloylmorpholine)-*block*-(*N*-acryloylazocane)] (PAM-PAH), where the numbers in parentheses denote the weight fraction of each block. [c] δ indicates the segregation factor, where $R = D/2 \approx N_t^{\delta}$. [d] Z indicates the aggregation number ($Z \approx N_t^{\alpha}$), where $\delta = (\alpha + 1)/3$.

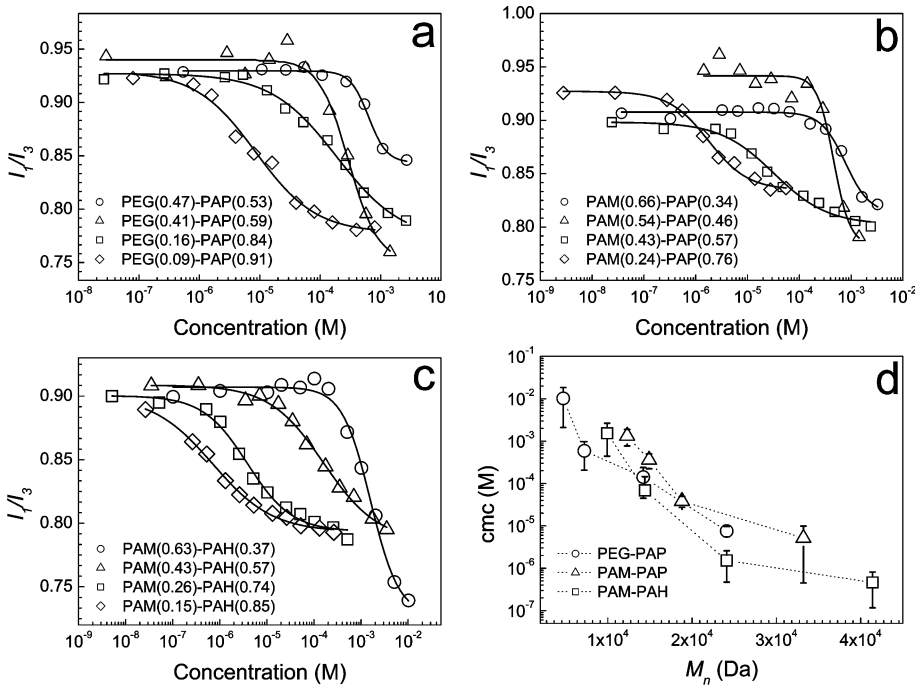

Figure 5. Critical micelle concentrations (cmcs) determined by pyrene method for the a) poly[(ethylene glycol)-*block*-(*N*-acryloylpiperidine)] (PEG-PAP), (b) poly[(*N*-acryloylmorpholine)-*block*-(*N*-acryloylpiperidine)] (PAM-PAP), (c) poly[(*N*-acryloylmorpholine)-*block*-(*N*-acryloylazocane)] (PAM-PAH) series, where the numbers in parentheses denote the weight fraction of each block, and (d) cmc plotted vs $\overline{M}_n$ in a semilogarithmic scale (error bar: SD for $n = 3$). Graphs from part a to part c represent one representative example out of triplicates.

We considered comparing two pairs of block copolymers in terms of (1) hydrophilicity comparison (PEG vs PAM) and (2) hydrophobicity comparison (PAP vs PAH). From the above interpretations, we believe that the hydrophile PAM segregates with PAP less than does the hydrophile PEG, which suggests that PAM possess less hydrophilicity as PEG. Vice versa, if one compares the hydrophobicity of PAP to PAH with a common hydrophilic block, PAM, PAH reveals itself to be substantially more hydrophobic. As for two pairs with similar molecular weight, PAM(0.43)-PAP(0.57) (18.8 kDa) vs PAM-(0.26)-PAH(0.74) (24.1 kDa), PAM(0.43)-PAP(0.57) was found to exist at the WSL, while PAM(0.26)-PAH(0.74) was positioned in the SSR. This was also found with PAM(0.24)-PAP-(0.76) (33.2 kDa) and PAM(0.15)-PAH(0.85) (41.4 kDa). Speculating how cmc correlates with molecular weight, one notices the PAM-PAP series is generally placed higher than the PAM-PAH series in overall, especially when compared between two pairs; PAM(0.66)-PAP(0.34) vs PAM(0.63)-PAH-(0.37) and PAM(0.54)-PAP(0.46) vs PAM(0.43)-PAH(0.57). This discussion leads us to conclude that the PAH block segregates PAM more strongly than PAP does, and it coincides well with our initial speculation from its structure.

3.6. *in vitro* Release of Everolimus from PAM-PAH Micelles. Everolimus is a mammalian target of rapamycin (mTOR) inhibitor widely used in cardiac transplantation and recently it has been also used for the treatment of cardiovascular diseases associated with drug-eluting stent. In this study, everolimus was loaded in the micelles of PAM(0.15)-PAH-(0.85). As an example of a hydrophobic drug, its encapsulation efficiency was 60 ± 7.8%. In 3 weeks, 87% of everolimus loaded was released, as shown in Figure 6, demonstrating that PAM-PAH micelles can be suitable drug carrier releasing hydrophobic drugs over a long time span.

$$\frac{M_t}{M_{\inf}} = \frac{M_b}{M_{\inf}} + kt^n \qquad (6)$$

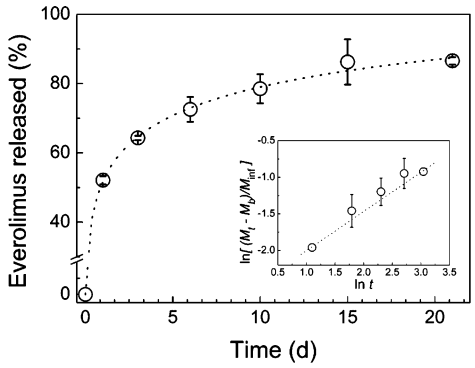

Figure 6. Release profile of everolimus from PAM(0.15)-PAH(0.85) micelles in PBS (pH 7.4, 10 mM) at 37 °C. PAM-PAH denotes poly-[(*N*-acryloylmorpholine)-*block*-(*N*-acryloylazocane)] diblock copolymer. The inset represents the fitted line according to the eq 6, where M_t denotes the amount of everolimus released at time t, M_{inf} denotes the amount of everolimus released at infinite time, M_b denotes the initially burst amount of everolimus, and n denotes the release exponent.

Table 6. Hydrodynamic Diameter and Encapsulation Efficiency of Everolimus-loaded Micelles Formed from Poly[(*N*-acryloylmorpholine)-*block*-(*N*-acryloylazocane)] (PAM-PAH) Diblock Copolymer[a,b]

before loading (nm)	after loading (nm)	encapsulation efficiency (%)[c]
43 ± 0.1	52 ± 1.8	60 ± 7.8

[a] Solvent evaporation method was used to encapsulate the drug in PAM(0.15)-PAH(0.85) micelles. [b] Mean ± SD for $n = 3$. [c] Encapsulation efficiency (%) = (the actual amount of loaded drug)/(the amount of total drug attempted) × 100. n denotes the release exponent and k denotes the release constant.

Table 7. Calculated Kinetic Parameters of the Release of Everolimus from PAM(0.15)-PAH(0.85) Micelles[a,b]

n	k
0.55± 0.047	2.50 ± 0.170

[a] Data were fitted by eq 6. [b] Mean ± SD for $n = 3$. PAM-PAH denotes [(*N*-acryloylmorpholine)-*block*-(*N*-acryloylazocane)] diblock copolymer.

where M_t is the amount of everolimus released at time t, M_{inf} is the amount of everolimus released at infinite time, M_b is the initially burst amount of everolimus, k is the release constant, and n is the release exponent.

The experimental data were fitted using eq 6 to evaluate release constant and release exponent. In our study, n was evaluated as 0.55 ± 0.047 as listed in Table 7. As Siepmann and Peppas reported,[83] n varies between 0.43 (diffusion-based release) and 0.87 (degradation-based release). In our result for n, the value closer to 0.43 implies that everolimus release is mostly driven by the diffusion from the cores of micelles, in agreement with the nondegradable properties of PAM-PAH micelles. A similar value was observed from hydrogel nanoparticles loading doxorubicin as reported by Missirlis et al.[84]

4. Conclusion

We describe here a strategy to prepare various amphiphilic block copolymeric poly(acrylamide)s by RAFT polymerization. Such macroamphiphiles were obtained with morpholine, piperidine, and azocane side groups to generate hydrophilicity, from PAM block, or hydrophobicity, from PAP and PAH blocks. Diblock copolymers formed from these building blocks self-assembled into spherical micelles or polymersomes in aqueous conditions and revealed different segregating behavior as studied in terms of cmc measurements and several segregating models. PAM shows similar behavior as the better studied PEG with respect to the size of aggregates and segregation behavior. In addition, PAH was revealed as a more segregating hydrophobe than PAP, corresponding to the greater number of methylene groups on the side group of the acrylamide monomer, provide higher hydrophobicity. PAM-PAH micelles could load everolimus, a hydrophobic model drug with superior encapsulation efficiency and the drug was released over 3 weeks in a slow releasing pattern. These self-assembling macroamphiphiles may have applications in drug delivery systems, as demonstrated with model drug incorporation, whether to contain a hydrophobic payload or to display surface biofunctionality or linked drugs.

Acknowledgment. The authors thank Dr. Quoc Tuan Nguyen at Laboratoire des Polymers (Prof. H. -A. Klok) in EPFL, and Mr. Johann Fitz and Dr. Dierk Roessner in Wyatt GmbH (Dernbach, Germany) for the SEC experiments with MALS detector and their valuable consultation.

Supporting Information Available: Figures showing ^{1}H NMR (400 MHz) spectra for acrylamide monomers and polymers and size exclusion chromatograms of diblock copolymers. This material is available free of charge via the Internet at http://pubs.acs.org.

Note Added after ASAP Publication. This article was published ASAP on February 5, 2008. Figure 5 has been replaced and numerous minor text changes have been made. The correct version was published on February 7, 2008.

References and Notes

(1) Torchilin, V. P. *J. Controlled Release* **2001**, *73*, 137−172.
(2) Kataoka, K.; Kwon, G. S.; Yokayama, M.; Okano, T.; Sakurai, Y. *J. Controlled Release* **1993**, *24*, 119−132.
(3) Kataoka, K.; Harada, A.; Nagasaki, Y. *Adv. Drug Delivery Rev.* **2001**, *47*, 113−131.
(4) Hubbell, J. A. *Science* **2003**, *300*, 595−596.
(5) Zhang, Y.; Guo, S.; Lu, C.; Liu, L.; Li, Z.; Gu, J. *J. Polym. Sci., Part A: Polym. Chem.* **2007**, *45*, 605−613.
(6) Savic, R.; Luo, L.; Eisenberg, A.; Maysinger, D. *Science* **2003**, *300*, 615−618.
(7) Zhang, L.; Eisenberg, A. *Science* **1995**, *268*, 1728−1731.
(8) Dalhaimer, P.; Bates, F. S.; Discher, D. E. *Macromolecules* **2003**, *36*, 6873−6877.
(9) Discher, D. E.; Eisenberg, A. *Science* **2002**, *297*, 967−973.
(10) Discher, B. M.; Won, Y. Y.; Ege, D. S.; Lee, J. C. M.; Bates, F. S.; Discher, D. E.; Hammer, D. A. *Science* **1999**, *284*, 1143−1146.
(11) Castelletto, V.; Hamley, I. W. *Polym. Adv. Technol.* **2006**, *17*, 137−144.
(12) Torchilin, V. P. *Pharm. Res.* **2007**, *V24*, 1−16.
(13) Vicent, M. J.; Duncan, R. *Trends Biotechnol.* **2006**, *24*, 39−47.
(14) Kwon, G. S.; Naito, M.; Yokoyama, M.; Okano, T.; Sakurai, Y.; Kataoka, K. *Pharm. Res.* **1995**, *V12*, 192−195.
(15) Yokoyama, M.; Miyauchi, M.; Yamada, N.; Okano, T.; Sakurai, Y.; Kataoka, K.; Inoue, S. *Cancer Res.* **1990**, *50*, 1693−1700.
(16) Andersson, L.; Davies, J.; Duncan, R.; Ferruti, P.; Ford, J.; Kneller, S.; Mendichi, R.; Pasut, G.; Schiavon, O.; Summerford, C.; Tirk, A.; Veronese, F. M.; Vincenzi, V.; Wu, G. *Biomacromolecules* **2005**, *6*, 914−926.
(17) Bae, Y.; Nishiyama, N.; Fukushima, S.; Koyama, H.; Yasuhiro, M.; Kataoka, K. *Bioconjugate Chem.* **2005**, *16*, 122−130.
(18) Zhang, C.; Ding, Y.; Yu, L.; Ping, Q. *Colloids Surf. B* **2007**, *55*, 192−199.
(19) Koizumi, F.; Kitagawa, M.; Negishi, T.; Onda, T.; Matsumoto, S.-I.; Hamaguchi, T.; Matsumura, Y. *Cancer Res.* **2006**, *66*, 10048−10056.
(20) Opanasopit, P.; Ngawhirunpat, T.; Chaidedgumjorn, A.; Rojanarata, T.; Apirakaramwong, A.; Phongying, S.; Choochottiros, C.; Chirachanchai, S. *Eur. J. Pharmacol. Biopharm.* **2006**, *64*, 269−276.
(21) Kawano, K.; Watanabe, M.; Yamamoto, T.; Yokoyama, M.; Opanasopit, P.; Okano, T.; Maitani, Y. *J. Controlled Release* **2006**, *112*, 329−332.
(22) Shuai, X.; Merdan, T.; Schaper, A. K.; Xi, F.; Kissel, T. *Bioconjugate Chem.* **2004**, *15*, 441−448.
(23) Lee, S. C.; Huh, K. M.; Lee, J.; Cho, Y. W.; Galinsky, R. E.; Park, K. *Biomacromolecules* **2007**, *8*, 202−208.

(24) Liggins, R. T.; Burt, H. M. *Adv. Drug Delivery Rev.* **2002**, *54*, 191−202.
(25) Seow, W. Y.; Xue, J. M.; Yang, Y.-Y. *Biomaterials* **2007**, *28*, 1730−1740.
(26) Wang, Y.; Yu, L.; Han, L.; Sha, X.; Fang, X. *Int. J. Pharm.* **2007**, *337*, 63−73.
(27) Francis, M. F.; Lavoie, L.; Winnik, F. M.; Leroux, J.-C. *Eur. J. Pharmacol. Biopharm.* **2003**, *56*, 337−346.
(28) Aliabadi, H. M.; Elhasi, S.; Mahmud, A.; Gulamhusein, R.; Mahdipoor, P.; Lavasanifar, A. *Int. J. Pharm.* **2007**, *329*, 158−165.
(29) Aliabadi, H. M.; Mahmud, A.; Sharifabadi, A. D.; Lavasanifar, A. *J. Controlled Release* **2005**, *104*, 301−311.
(30) Bontha, S.; Kabanov, A. V.; Bronich, T. K. *J. Controlled Release* **2006**, *114*, 163−174.
(31) Nishiyama, N.; Kataoka, K. *J. Controlled Release* **2001**, *74*, 83−94.
(32) Forrest, M. L.; Won, C.-Y.; Malick, A. W.; Kwon, G. S. *J. Controlled Release* **2006**, *110*, 370−377.
(33) Satturwar, P.; Eddine, M. N.; Ravenelle, F.; Leroux, J.-C. *Eur. J. Pharmacol. Biopharm.* **2007**, *65*, 379−387.
(34) Roberts, M. J.; Bentley, M. D.; Harris, J. M. *Adv. Drug Delivery Rev.* **2002**, *54*, 459−476.
(35) Tosatti, S.; Paul, S. M. D.; Askendal, A.; VandeVondele, S.; Hubbell, J. A.; Tengvall, P.; Textor, M. *Biomaterials* **2003**, *24*, 4949−4958.
(36) Bearinger, J. P.; Terrettaz, S.; Michel, R.; Tirelli, N.; Vogel, H.; Textor, M.; Hubbell, J. A. *Nat. Mater.* **2003**, *2*, 259−264.
(37) Kataoka, K.; Matsumoto, T.; Yokoyama, M.; Okano, T.; Sakurai, Y.; Fukushima, S.; Okamoto, K.; Kwon, G. S. *J. Controlled Release* **2000**, *64*, 143−153.
(38) Yasugi, K.; Nagasaki, Y.; Kato, M.; Kataoka, K. *J. Controlled Release* **1999**, *62*, 89−100.
(39) Sartore, L.; Peroni, I.; Ferruti, P.; Latini, R.; Bernasconi, R. *J. Biomater. Sci. Polym. Ed.* **1997**, *8*, 741−754.
(40) Caliceti, P.; Schiavon, O.; Veronese, F. M. *Bioconjugate Chem.* **2001**, *12*, 515−522.
(41) Torchilin, V. P.; Trubetskoy, V. S.; Whiteman, K. R.; Caliceti, P.; Ferruti, P.; Veronese, F. M. *J. Pharm. Sci.* **1995**, *84*, 1049−1053.
(42) Torchilin, V. P.; Shtilman, M. I.; Trubetskoy, V. S.; Whiteman, K.; Milstein, A. M. *Biochim. Biophys. Acta* **1994**, *1195*, 181−184.
(43) Ranucci, E.; Spagnoli, G.; Sartore, L.; Ferruti, P.; Caliceti, P.; Schiavon, O.; Veronese, F. M. *Macromol. Chem. Phys.* **1994**, *195*, 3469−3479.
(44) D'Agosto, F.; Charreyre, M. T.; Melis, F.; Mandrand, B.; Pichot, C. *J. Appl. Polym. Sci.* **2003**, *88*, 1808−1816.
(45) D'Agosto, F.; Hughes, R.; Charreyre, M. T.; Pichot, C.; Gilbert, R. G. *Macromolecules* **2003**, *36*, 621−629.
(46) Favier, A.; Charreyre, M.-T.; Pichot, C. *Polymer* **2004**, *45*, 8661−8674.
(47) Favier, A.; Ladaviere, C.; Charreyre, M. T.; Pichot, C. *Macromolecules* **2004**, *37*, 2026−2034.
(48) Favier, A.; Charreyre, M. T.; Chaumont, P.; Pichot, C. *Macromolecules* **2002**, *35*, 8271−8280.
(49) Perrier, S.; Davis, T. P.; Carmichael, A. J.; Haddleton, D. M. *Chem. Commun.* **2002**, 2226−2227.
(50) Convertine, A. J.; Ayres, N.; Scales, C. W.; Lowe, A. B.; McCormick, C. L. *Biomacromolecules* **2004**, *5*, 1177−1180.
(51) Millard, P.-E.; Barner, L.; Stenzel, M. H.; Davis, T. P.; Barner-Kowollik, C.; Müller, A. H. E. *Macromol. Rapid Commun.* **2006**, *27*, 821−828.
(52) Relogio, P.; Charreyre, M.-T.; Farinha, J. P. S.; Martinho, J. M. G.; Pichot, C. *Polymer* **2004**, *45*, 8639−8649.
(53) Chiefari, J.; Chong, Y. K.; Ercole, F.; Krstina, J.; Jeffery, J.; Le, T. P. T.; Mayadunne, R. T. A.; Meijs, G. F.; Moad, C. L.; Moad, G.; Rizzardo, E.; Thang, S. H. *Macromolecules* **1998**, *31*, 5559−5562.
(54) Perrier, S.; Takolpuckdee, P. *J. Polym. Sci., Part A: Polym. Chem.* **2005**, *43*, 5347−5393.
(55) Thomas, D. B.; Convertine, A. J.; Myrick, L. J.; Scales, C. W.; Smith, A. E.; Lowe, A. B.; Vasilieva, Y. A.; Ayres, N.; McCormick, C. L. *Macromolecules* **2004**, *37*, 8941−8950.
(56) Lowe, A. B.; McCormick, C. L. *Aust. J. Chem.* **2002**, *55*, 367−379.
(57) Matyjaszewski, K.; Xia, J. *Chem. Rev.* **2001**, *101*, 2921−2990.
(58) Jewrajka, S. K.; Mandal, B. M. *Macromolecules* **2003**, *36*, 311−317.
(59) Senoo, M.; Kotani, Y.; Kamigaito, M.; Sawamoto, M. *Macromolecules* **1999**, *32*, 8005−8009.
(60) Xiao, D.; Wirth, M. J. *Macromolecules* **2002**, *35*, 2919−2925.
(61) Hoshino, K.; Taniguchi, M.; Kitao, T.; Morohashi, S.; Sasakura, T. *Biotechnol. Bioeng.* **1998**, *60*, 568−579.
(62) Bennett, A. E.; Rienstra, C. M.; Auger, M.; Lakshmi, K. V.; Griffin, R. G. *J. Chem. Phys.* **1995**, *103*, 6951−6958.
(63) Parrod, J.; Elles, J. C. R. *C. R. Hebd. Seances Acad. Sci.* **1956**, *243*, 1040−1042.
(64) Perrier, S.; Takolpuckdee, P.; Westwood, J.; Lewis, D. M. *Macromolecules* **2004**, *37*, 2709−2717.
(65) Cerritelli, S.; Fontana, A.; Velluto, D.; Adrian, M.; Dubochet, J.; De Maria, P.; Hubbell, J. A. *Macromolecules* **2005**, *38*, 7845−7851.
(66) Butler, K.; Thomas, P. R.; Tyler, G. J. *J. Polym. Sci.* **1960**, *48*, 357−366.
(67) Khousakoun, E.; Gohy, J.-F.; Jerome, R. *Polymer* **2004**, *45*, 8303−8310.
(68) Shi, L. J.; Chapman, T. M.; Beckman, E. J. *Macromolecules* **2003**, *36*, 2563−2567.
(69) Ushakova, V.; Panarin, E.; Ranucci, E.; Bignotti, F.; Ferruti, P. *Macromol. Chem. Phys.* **1995**, *196*, 2927−2939.
(70) Snyder, L. R. *J. Chromatogr. A* **1974**, *92*, 223−230.
(71) Save, N. S.; Jassal, M.; Agrawal, A. K. *J. Appl. Polym. Sci.* **2005**, *95*, 672−680.
(72) Yu, Y.; Eisenberg, A. *J. Am. Chem. Soc.* **1997**, *119*, 8383−8384.
(73) Marinov, G.; Michels, B.; Zana, R. *Langmuir* **1998**, *14*, 2639−2644.
(74) Su, Y. L.; Wei, X. F.; Liu, H. Z. *Langmuir* **2003**, *19*, 2995−3000.
(75) Varade, D.; Sharma, R.; Aswal, V. K.; Goyal, P. S.; Bahadur, P. *Eur. Polym. J.* **2004**, *40*, 2457−2464.
(76) Matsumoto, K.; Ishizuka, T.; Harada, T.; Matsuoka, H. *Langmuir* **2004**, *20*, 7270−7282.
(77) Matsuoka, H.; Maeda, S.; Kaewsaiha, P.; Matsumoto, K. *Langmuir* **2004**, *20*, 7412−7421.
(78) Patist, A.; Bhagwat, S. S.; Penfield, K. W.; Aikens, P.; Shah, D. O. *J. Surfactants Deterg.* **2000**, *V3*, 53−58.
(79) Kaewsaiha, P.; Matsumoto, K.; Matsuoka, H. *Langmuir* **2005**, *21*, 9938−9945.
(80) Forster, S.; Zisenis, M.; Wenz, E.; Antonietti, M. *J. Chem. Phys.* **1996**, *104*, 9956−9970.
(81) Bates, F. S.; Fredrickson, G. H. *Annu. Rev. Phys. Chem.* **1990**, *41*, 525−557.
(82) Nyrkova, I. A.; Khokhlov, A. R.; Doi, M. *Macromolecules* **1993**, *26*, 3601−3610.
(83) Siepmann, J.; Peppas, N. A. *Adv. Drug Delivery Rev.* **2001**, *48*, 139−157.
(84) Missirlis, D.; Kawamura, R.; Tirelli, N.; Hubbell, J. A. *Eur. J. Pharmacol. Sci.* **2006**, *29*, 120−129.

MA071710T